

Nanocomputing by Field-Coupled Nanomagnets

György Csaba, Alexandra Imre, Gary. H. Bernstein, Wolfgang Porod, *Fellow, IEEE*, and Vitali Metlushko

Abstract—We demonstrate through simulations the feasibility of using magnetically coupled nanometer-scale ferromagnetic dots for digital information processing. Microelectronic circuits provide the input and output of the magnetic nanostructure, but the signal is processed via magnetic dot–dot interactions. Logic functions can be defined by the proper placements of dots. We introduce a SPICE macromodel of interacting nanomagnets and use this tool to design and simulate the proposed nanomagnet logic units. This SPICE model allows us to simulate such magnetic information processing devices within the same framework as conventional electronic circuits.

Index Terms—Magnetic memories, micromagnetic design, patterned magnetic media, quantum-dot cellular automata, single-domain approximation, SPICE macromodel.

I. INTRODUCTION

THE computer data storage industry has been dominated for several decades by thin magnetic film technologies. Recently, patterned magnetic media on the deep submicron and nanoscale have opened the prospect of novel storage device structures [1]. Using an individual ferromagnetic dot to represent a single bit of information promises to increase the capacity of hard disk drives (HDDs) by one or two orders of magnitude. Magnetic random access memory (MRAM) devices also have the potential to revolutionize the data storage industry because they offer lower energy dissipation, higher speed, and larger storage density than current dynamic RAM devices.

In such patterned magnetic media, each magnetic storage particle is individually addressed by either read–write (RW) heads (as in the case of HDDs) or by crossing electric wires (as in the case of MRAMs). The storage capacity is limited by the RW apparatus and not by the size of the magnetic dot itself. Moreover, dipolar interaction between neighboring magnetic particles may cause loss of stored information and so limit the packing density of dots.

The aim of this work is to take advantage of these otherwise undesirable dipolar interactions and to exploit them for providing interconnectivity in large arrays of magnetic dots. This eliminates the need for individual access to each dot. The RW apparatus is necessary only at the periphery of the array where it controls the state of the “input dots” and reads out the

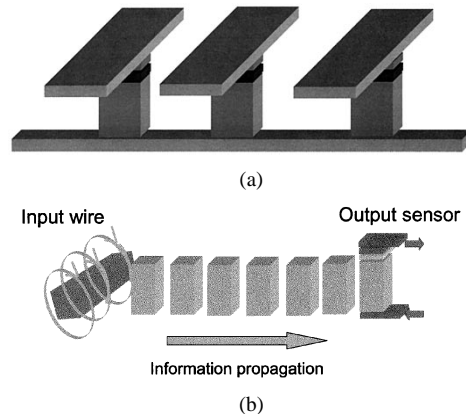


Fig. 1. (a) Individual access of nanomagnets in an MRAM device. (b) Field-coupled structure.

“output dots.” In the interior of the array, information propagates entirely through magnetic dot–dot interactions. This concept of providing local interconnectivity through physical interactions is similar to the quantum-dot cellular automata (QCA) scheme [2], applied to magnetic interactions [3]. This concept is illustrated in Fig. 1, where a schematic MRAM structure (each dot contacted by wires) is compared to a line of magnetically coupled dots.

Magnetic interactions can be used not only for the propagation of information, but to perform signal processing tasks as well. If the interaction between neighboring dots is sufficiently strong, then the state of each dot can be uniquely determined by the state of its neighbors and its magnetization history. We will demonstrate the design of geometries to realize elementary Boolean logic functions.

The well-established theory of micromagnetics [4], [5] describes the behavior of ferromagnetic particles. However, this theory is too complex and computationally intensive to be useful for purposes of designing large dot arrays. We have, therefore, developed a SPICE macromodel for the simulation of interacting nanomagnet arrays, which also allows us to treat these arrays embedded in microelectronic circuits.

This SPICE model is based on the single-domain approximation (SDA), which is a limiting case of the micromagnetic equations for nanometer-size particles. Based upon this SPICE model, we will demonstrate two examples of simple nanomagnet circuits, namely, a wire and a majority-logic gate.

To our knowledge, relatively little work has been done on SPICE modeling of magnetic nanostructures. Macromodels have been developed for giant magnetoresistance (GMR) memory cells [6], but these models incorporate hysteresis effects only in a phenomenological way. We believe that our work is the first that uses SPICE as a physics-based micromagnetics

Manuscript received June 6, 2002; revised August 19, 2002. This work was supported in part by grants from the Office of Naval Research and the W.M. Keck Foundation. This paper is based on work presented at the 2002 Silicon Nanoelectronics Workshop, Honolulu, HI, June 2002.

G. Csaba, A. Imre, G. H. Bernstein, and W. Porod are with the Center for Nano Science and Technology, Department of Electrical Engineering, University of Notre Dame, Notre Dame IN 46556 USA (e-mail: Gyorgy.Csaba.1@nd.edu).

V. Metlushko is with the Department of Electrical Engineering and Computer Science, University of Illinois, Chicago, IL 60607 USA.

Digital Object Identifier 10.1109/TNANO.2002.807380

simulator, which opens the way to efficient simulation and design of nanomagnet structures integrated in microelectronic circuits.

II. SPICE MODEL OF INTERACTING NANOMAGNETS

A. Single-Domain Approximation

Sufficiently small magnetic particles are known to exhibit single-domain behavior, while larger particles show complex domain structures. Typically, permalloy dots with dimensions on the order of 100 nm display single-domain behavior. Here, we will briefly outline this approximation, and the full details and limitations of this model will be discussed in a forthcoming paper [7].

The single-domain Landau–Lifschitz equation describes how the magnetization of a ferromagnetic particle $\mathbf{M}^{(i)}(t)$ changes under the influence of an effective field $\mathbf{H}_{\text{eff}}^{(i)}(t)$

$$\frac{d\mathbf{M}^{(i)}(t)}{dt} = -\gamma\mathbf{M}^{(i)}(t) \times \mathbf{H}_{\text{eff}}^{(i)}(t) - \frac{\alpha\gamma}{M_s} \left[\mathbf{M}^{(i)}(t) \times \left(\mathbf{M}^{(i)}(t) \times \mathbf{H}_{\text{eff}}^{(i)}(t) \right) \right]. \quad (1)$$

This effective field can be calculated from

$$\mathbf{H}_{\text{eff}}^{(i)} = \mathbf{N}^{(i)}\mathbf{M}^{(i)} + \sum_{j=\text{neighbors}} \mathbf{C}^{(ij)}\mathbf{M}^{(j)} + \mathbf{H}_{\text{Zeeman}}^{(i)} \quad (2)$$

where $\mathbf{N}^{(i)}$ is the demagnetization tensor of dot i which takes into account the shape anisotropy of the dot. Analytical formulas are available for ellipsoids and prism-shaped particles [4], [8]. As an illustration, for a prolate ellipsoid with axes a, c, c , the matrix is diagonal and its elements are given by

$$\mathbf{N} = \begin{bmatrix} N_a & 0 & 0 \\ 0 & N_c & 0 \\ 0 & 0 & N_c \end{bmatrix} \\ \alpha = \frac{c}{a} < 1 \\ N_a = \frac{\alpha^2}{\alpha^2 - 1} \left[1 - \frac{1}{\sqrt{\alpha^2 - 1}} \arcsin \left(\frac{\sqrt{\alpha^2 - 1}}{\alpha} \right) \right] \\ N_c = \frac{1}{2} (1 - N_a). \quad (3)$$

The matrix $\mathbf{C}^{(ij)}$ describes the coupling between nanomagnets i and j and can be calculated from the point-dipole approximation

$$\mathbf{C}^{(ij)} = \frac{V^{(j)}}{4\pi r_{ij}^3} \begin{bmatrix} 3\hat{r}_x^2 - 1 & 3\hat{r}_x\hat{r}_y & 3\hat{r}_x\hat{r}_z \\ 3\hat{r}_y\hat{r}_x & 3\hat{r}_y^2 - 1 & 3\hat{r}_y\hat{r}_z \\ 3\hat{r}_z\hat{r}_x & 3\hat{r}_z\hat{r}_y & 3\hat{r}_z^2 - 1 \end{bmatrix}. \quad (4)$$

Here, r_{ij} is the distance between the dots and $\hat{\mathbf{r}} = (\hat{r}_x, \hat{r}_y, \hat{r}_z)$ is the unit vector pointing from magnet i to magnet j . $V^{(j)}$ is the volume of magnet j . Both the \mathbf{N} and \mathbf{C} matrices are constants for a given geometry.

$\mathbf{H}_{\text{Zeeman}}$ is the applied external field, which is split into two parts

$$\mathbf{H}_{\text{Zeeman}} = \mathbf{H}_{\text{Ext}} + \mathbf{H}_{\text{Current}} \quad (5)$$

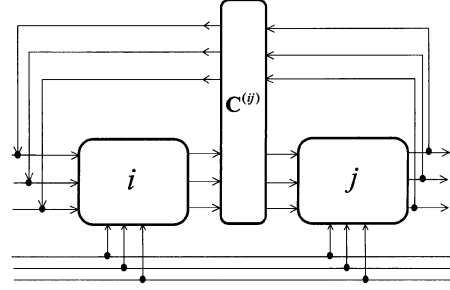


Fig. 2. Circuit blocks of two coupled nanomagnets i and j .

where \mathbf{H}_{Ext} is a homogenous external field and $\mathbf{H}_{\text{Current}}$ is the field generated by the input wires.

For an array of nanomagnets, these formulas lead to a system of coupled ordinary differential equations (ODEs), with three equations per nanomagnet. We will directly proceed to the numerical solution by SPICE.

B. Dynamic Circuit Model

An equivalent-circuit model of the above ODEs can be constructed by formally viewing the normalized magnetization components $\mathbf{m} = \mathbf{M}/M_s$ and the magnetic fields as generalized “currents.” The three components of the Landau–Lifschitz equations can be written as

$$\frac{dm_x(t)}{dt} = \gamma (H_z m_y - H_y m_z) - \alpha\gamma (H_y m_x m_y - H_x m_y^2 - H_x m_z^2 + H_z m_x m_z) \\ \frac{dm_y(t)}{dt} = \gamma (H_x m_z - H_z m_x) - \alpha\gamma (H_z m_y m_z - H_y m_z^2 - H_y m_x^2 + H_x m_x m_y) \\ \frac{dm_z(t)}{dt} = \gamma (H_y m_x - H_x m_y) - \alpha\gamma (H_x m_z m_x - H_z m_x^2 - H_z m_y^2 + H_y m_y m_z) \quad (6)$$

where H_x, H_y, H_z are the components of the effective field in units of the saturation magnetization M_s .

The circuit model of a nanomagnet is split into two subcircuits. The “dot circuit” models the behavior of an individual dot, based on (6) and parameterized with the demagnetization tensor, which accounts for the particle geometry. The “coupler circuit” provides the interaction field $\mathbf{C}^{(ij)}\mathbf{M}^{(j)}$ [see (2)] as parameterized with the coupling matrix, which depends upon the dot distances. It is usually sufficient to take into account interactions within the nearest-neighbor approximation.

As an illustration of the above equivalent-circuit model, consider two coupled nanomagnets. Fig. 2 shows the block diagram of the “circuit” which models coupled dots i and j , and the corresponding equivalent-dot-circuit model is displayed in Fig. 3. The control equations of the current-controlled voltage sources are defined by the right-hand side of (6).

The dot-circuit has current input, which represents the coupling fields and voltage input, which represents the external fields. This is a convenient feature of our model, which naturally provides the summation over the fields of neighboring dots by Kirchoff’s current law. \mathbf{H}_{Ext} is a separate voltage input and all

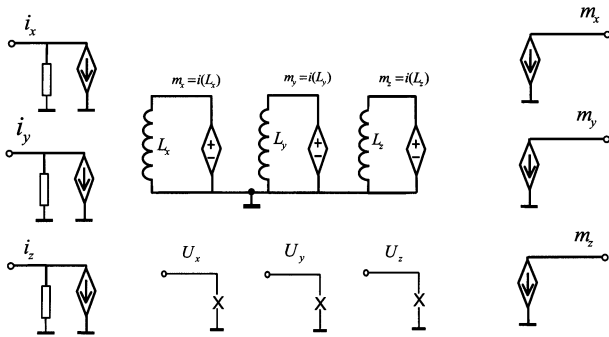


Fig. 3. Schematic diagram of the dot-circuit. The six-input three-output block directly simulates (6).

circuits experience the same \mathbf{H}_{Ext} due to the assumed homogeneity of the external (pumping) field.

C. Input and Output Circuits

The input to the nanomagnet structure is provided by electric currents (which generate the magnetic fields for the input dots) and the state of the output dots is read by magnetic field sensors (GMR or magnetic tunnel junction devices). The input coupler circuit simply generates a magnetic field (input current of a dot circuit) given by the Biot–Savart law

$$\mathbf{H}_{\text{current}} = \frac{\mathbf{I} \times \hat{\mathbf{r}}}{2\pi r}. \quad (7)$$

The output circuit simply consists of a field-dependent resistor, which represents the sensing device [9].

D. SPICE Implementation of Circuit Models

We implemented the above models in TSPICE. Other SPICE versions (like HSPICE) also work after some modification of the default time integration parameters. Transient simulation of simple structures, like the ones shown in the next section, took less than a minute on an average PC. This high efficiency enables the execution of time-consuming Monte Carlo simulations (distortion analysis) and investigation of relatively complex (few ten or hundred dot) structures.

III. EXAMPLES OF NANOMAGNET LOGIC DEVICES

A. Nanomagnet Wire

The nanomagnet wire is a line of coupled nanomagnets, where the state of each dot is determined by a single input signal. In this design, the wire is built from pillar-shaped permalloy dots ($N_z < N_x, N_y$). Shape anisotropy ensures that the stable zero-field magnetization of the dot is parallel to its longest axis (perpendicular to the surface). Digital information is represented by the z component (vertical) of the magnetization as schematically shown in Fig. 4. A logic value of “1” can be assigned to $m_z = 1$ and logical “0” to $m_z = -1$. An external magnetic field cycle is applied to drive the dots from an arbitrary initial state to the ordered final state. The layout and schematics of the operation are sketched in Fig. 4, while the result of the corresponding SPICE simulation is presented in Fig. 5.

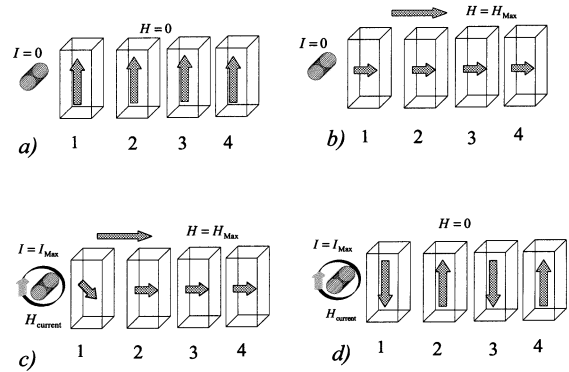


Fig. 4. Operating scheme of the nanowire. (a) Initial configuration. (b) High-field state before and (c) after the application of the input. (d) Final ordered state.

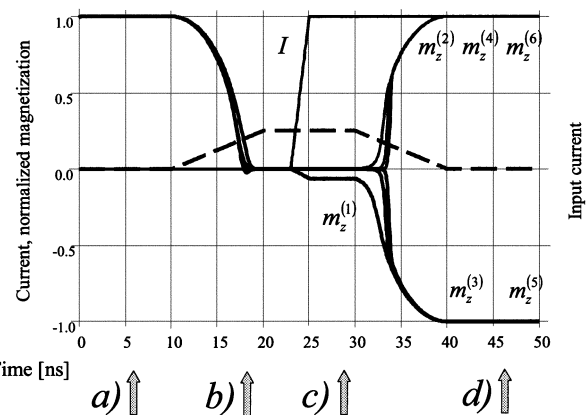


Fig. 5. SPICE simulation of the nanowire. The driver current and the m_z components are shown. The phases (a), (b), (c), (d) corresponds to schematics of Fig. 4. The dashed line is the pump field.

We assume that initially all dots are magnetized in the same direction [Fig. 4(a)]. An external magnetic pumping field is then applied. During the first clock phase [Fig. 4(b)], the “memory” of the initial state is “erased” by aligning all dots parallel to this strong external field, regardless of their magnetization history. In the second phase [Fig. 4(c)], the input current is switched, which influences the magnetization of the input dot. In the third phase [Fig. 4(d), as the clock field is adiabatically lowered], the effect of the weak input signal is amplified and propagates through the structure, resulting in an antiferromagnetically ordered state determined by the input.

B. Magnetic Majority Gate

The majority gate is the basic logic building block of nanomagnet circuits, just as for the electronic QCA versions. The layout of a magnetic majority gate with an output wire segment is sketched in Fig. 6. The input dots are labeled by 2, 3, and 4. The majority gate is clocked by an external field in a similar way to the nanowire. By the end of the pumping cycle, dot 1 will be antiparallel with the majority of its neighbors. If one of the input dots is in logical “1” state, the dot realizes a logical NOR function between the other two inputs and the output, and if one input is in logical “0”, then the gate computes the NAND function.

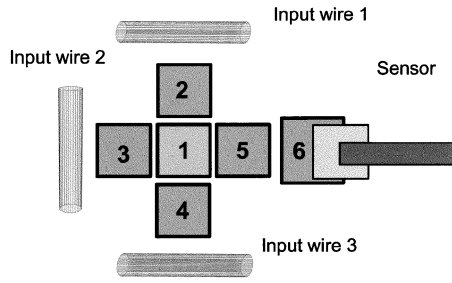


Fig. 6. Physical layout of the majority gate. The input dots (dot 2, 3, 4) are driven by electric wires and the result of the computation is represented by dot 6.

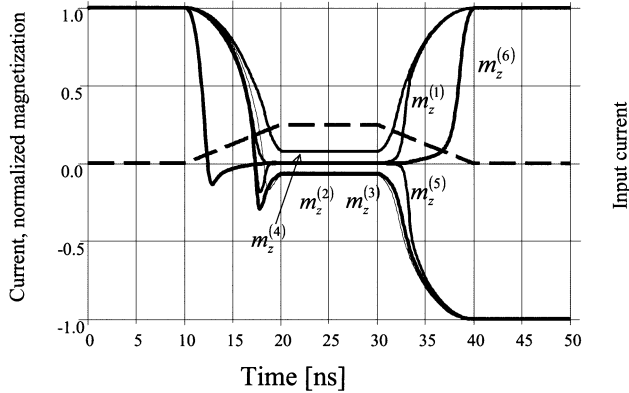


Fig. 7. SPICE simulation of the magnetic majority gate. The currents correspond to the perpendicular magnetization of the dots. The dashed line is the pump field.

The SPICE simulation of the majority gate for a particular input combination is shown in Fig. 7. Note that the geometry parameters of dot 6 are different from other dots in the structure. It assures that this dot is the first dot to make the transition to the $m_z = 0$ state and the last to switch back to a definite logic value. This fact defines dot 6 as the output of the structure.

C. Validity of the SDA for Circuit Simulations

Since it is not possible to give exact and general criteria for the validity of the SDA, one always has to verify it against micromagnetic simulations and experimental data. We performed detailed three-dimensional simulations [10] with the public-domain micromagnetics object-oriented micromagnetic framework (OOMMF) code [11]. The simulated behavior of subhundred-nanometer-size dots showed almost perfect agreement with the SDA results. For larger size or odd-shaped dots, the model had to be fitted to more sophisticated simulations, but simple structures (like the wire and the majority gate) work qualitatively the same way as expected from the single-domain model.

Note that the above circuit model correctly describes the fast transient magnetization dynamics of the dots. In Figs. 5 and 7, the time scales are very long compared to the subnanosecond spin precession times, and that is why the oscillating magnetization behavior is not visible.

IV. SUMMARY AND OUTLOOK

In this paper, we utilized SPICE for solving micromagnetic problems and we applied this tool to simulate the behavior of

systems of strongly coupled nanomagnets. The aim of this paper was to demonstrate that it is possible to perform signal-processing tasks with magnetic nanostructures and efficient computer-aided design tools can be developed in order to design structures of higher complexity.

In principle, the logic set shown in the previous section is satisfactory to realize any kind of Boolean logic function. Since the switching behavior of dots depends on their geometry parameters, a homogeneous external field can be designed to target specific dots in a larger array. (This eliminates the need for complex clocking circuits which are required for electronic QCA.) In a forthcoming publication [7], we will show how one can take advantage of this fact for realizing sequential (clocked) logic circuits. The clocked operation can eliminate unpredictable metastable states as well.

The SPICE macromodel presented here corresponds to only one level in the hierarchy of magnetic modeling. When only quasi-static behavior is of interest, nanomagnets can be fully characterized by their hysteresis curves, and the dot circuit of Fig. 3 can be substituted by a nonlinear static circuit. Besides its numerical efficiency, this approach is attractive from a theoretical viewpoint, because it gives an insight to the possible analogies between nonlinear electric circuit components and nonlinear magnetic behavior. There is also a possibility of overcoming the limitations of the SDA by introducing exchange coupling between magnetic particles.

Nanomagnet circuits, in principle, have numerous beneficial features. The power dissipation per bit operation is only a few tens of kiloteslas per bit operation, with relatively high speed (on the order of one hundred megahertz). The nanomagnet network itself is simple to realize and adds only a few technological steps to the standard silicon technology. The ultimate integration density is defined by the superparamagnetic limit and is probably above Terabit/inch² for devices operating at room temperature.

Given these attractive characteristics, we believe that nanomagnet logic devices might have promising applications in the future. These include intelligent magnetic field sensors, processing-in-memory-type architectures, or even a complex signal-processing unit, based entirely on magnetic field coupling.

ACKNOWLEDGMENT

The authors would like to thank Prof. A. Csurgay for fruitful discussions.

REFERENCES

- [1] G. A. Prinz, "Magnetoelectronics," *Science*, vol. 27, no. 282, pp. 1660–1663, Nov. 1998.
- [2] C. S. Lent, P. D. Tougaw, W. Porod, and G. H. Bernstein, "Quantum cellular automata," *Nanotechnol.*, pp. 49–57, Jan. 1993.
- [3] R. P. Cowburn and M. E. Welland, "Room temperature magnetic quantum cellular automata," *Science*, vol. 287, pp. 1466–1468, Feb. 2000.
- [4] A. Hubert and R. Schafer, *Magnetic Domains*. Berlin, Germany: Springer-Verlag, 1998.
- [5] A. Aharoni, *Introduction to Theory of Ferromagnetics*. Oxford, U.K.: Clarendon, 1996.
- [6] B. Das, W. C. Black, and A. V. Pohm, "Universal HSPICE macromodel for giant magnetoresistance memory bits," *IEEE Trans. Magn.*, vol. 36, pp. 2062–2072, July 2000.

- [7] G. Csaba and W. Porod, "Single-domain design of coupled ferromagnetic prisms and their applications as logic devices," *IEEE Trans. Nanotechnol.*, submitted for publication.
- [8] A. Aharoni, "Demagnetizing factors for rectangular ferromagnetic prisms," *J. Appl. Phys.*, vol. 83, no. 3432, 1998.
- [9] B. Dieny, V. S. Speriosu, S. S. P. Parkin, B. A. Gurnay, D. R. Wilhoit, and D. Mauri, "Giant magnetoresistance in soft magnetic multilayers," *Phys. Rev. B*, vol. 43, no. 1, pp. 1297–1300, Jan. 1991.
- [10] G. Csaba and W. Porod, "Simulation of field-coupled architectures based on magnetic dot arrays," *J. Comput. Electron. I*, vol. 1, pp. 87–91, Jan./Feb., 2002.
- [11] M. J. Donahue and D. G. Porter. OOMMF User's Guide, Version 1.0 Interagency Report NISTIR 6376. [Online]. Available: <http://math.nist.gov/oommf/>



György Csaba was born in Budapest, Hungary, in 1974. He received the M.S. degree from the Technical University of Budapest in 1998. He is currently working toward the Ph.D. degree at the University of Notre Dame, Notre Dame, IN.

His research interests are in modeling and simulation of nanoscale magnetic systems and exploring their applications for nonconventional (field-coupled) computing.



Alexandra Imre was born in Budapest, Hungary, in 1976. She received the M.S. degree from the Technical University of Budapest in 2001. She is currently working toward the Ph.D. degree at the Center for Nano Science and Technology, University of Notre Dame, Notre Dame, IN.

Her research interests are in the realization of nanomagnet structures by lithographic techniques and their characterization by magnetic force microscopy.



Gary H. Bernstein received the B.S. degree in electrical engineering from the University of Connecticut, Storrs, in 1979 and the M.S. degree in electrical engineering from Purdue University, West Lafayette, IN, in 1981. He received the Ph.D. degree from Arizona State University, Tempe, in 1987.

During the summers of 1979 and 1980, he was a Graduate Assistant at the Los Alamos National Laboratory, Los Alamos, CA, and in the summer of 1983, he interned at the Motorola Semiconductor Research and Development Laboratory, Phoenix, AZ. He was a Postdoctoral Fellow at Arizona State University in 1987. He joined the Department of Electrical Engineering, University of Notre Dame, Notre Dame, IN, in 1988 as an Assistant Professor and served as Director of the Microelectronics Laboratory from 1989 to 1998. He is currently Professor and Associate Chair of the Department of Electrical Engineering. He has authored or coauthored more than 90 publications in the areas of electron beam lithography, quantum electronics, ultrahigh-speed integrated circuits, reliability of ULSI components and microelectromechanical systems.

Dr. Bernstein received a National Science Foundation White House Presidential Teaching Award and is the recipient of a 2001 Notre Dame Kaneb Teaching Award.



Wolfgang Porod (M'86–SM'90–F'01) received the Diplom (M.S.) and Ph.D. degrees from the University of Graz, Austria, in 1979 and 1981, respectively.

He held postdoctoral positions at Colorado State University, Fort Collins, CO, from 1981 to 1983 and Arizona State University, Tempe, from 1983 to 1986. He joined the University of Notre Dame, Notre Dame, IN, in 1986. Currently, he is the Frank M. Freimann Professor of Electrical Engineering at the University of Notre Dame. His research interests are in the area of nanoelectronics, with particular

emphasis on new circuit concepts for novel nanoelectronic devices.



Vitali Metlushko received the B.S. and Ph.D. degrees from Moscow State University, Moscow, Russia, in 1984 and 1990, respectively, specializing in low-temperature physics and cryogenic engineering.

He is currently an Associate Professor with the Department of Electrical and Computer Engineering, University of Illinois, Chicago. His research interests include advanced recording media, new magnetic materials, and nanotechnology.